

properties of the HOMO and the LUMO (Fig. 4) should play a crucial role in ferromagnetism in doped hexaborides and CaB_2C_2 .

References and Notes

1. D. P. Young *et al.*, *Nature* **397**, 412 (1999).
 2. A. Hasegawa, A. Yanase, *J. Phys. C Solid State Phys.* **12**, 5431 (1979).

3. S. Massida, A. Continenza, T. M. de Pascale, R. Monnier, *Z. Phys.* **B102**, 83 (1997).
 4. M. E. Zhitomirsky, T. M. Rice, V. I. Anisimov, *Nature* **402**, 251 (1999).
 5. V. Barzkyin, L. P. Gor'kov, *Phys. Rev. Lett.* **84**, 1264 (2000).
 6. L. Balents, C. M. Varma, *Phys. Rev. Lett.* **84**, 2207 (2000).
 7. B. Albert, K. Schmitt, *Inorg. Chem.* **38**, 6159 (1999).
 8. T. Onimaru, H. Onodera, K. Ohyama, H. Yamauchi, Y. Yamaguchi, *J. Phys. Soc. Jpn.* **68**, 2287 (1999).

9. J. van Duijn, K. Suzuki, J. P. Attfield, *Angew. Chem. Int. Ed.* **39**, 365 (2000).
 10. H. J. Tromp *et al.*, *Phys. Rev. Lett.* **87**, 16401 (2001).
 11. P. Vonlanthen *et al.*, *Phys. Rev. B* **62**, 10076 (2000).
 12. Partially supported by a Grant-in-Aid for Science Research from the Ministry of Education, Culture, Sports, Science and Technology, Japan, and by a grant from the CREST.

10 April 2001; accepted 4 July 2001

Runaway Growth of Planetary Embryos Facilitated by Massive Bodies in a Protoplanetary Disk

Stephen J. Korkenkamp,^{1,2*} George W. Wetherill,² Satoshi Inaba²

About 30% of detected extrasolar planets exist in multiple-star systems. The standard model of planet formation cannot easily accommodate such systems and has difficulty explaining the odd orbital characteristics of most extrasolar giant planets. We demonstrate that the formation of terrestrial-size planets may be insulated from these problems, enabling much of the framework of the standard model to be salvaged for use in complex systems. A type of runaway growth is identified that allows planetary embryos to form by a combination of nebular gas drag and perturbations from massive companions—be they giant planets, brown dwarfs, or other stars.

The standard model of planet formation (*1-3*) begins with a protoplanetary disk of gas and dust orbiting a central protostar. Growth of terrestrial planets in such a disk is usually described in three stages: (i) accretion of dust particles into 10^{12} to 10^{18} g (kilometer-size) planetesimals in $\sim 10^4$ years (*4*); (ii) gravitational accumulation of planetesimals through a process known as “runaway growth” (*5*), which produces 10^{26} to 10^{27} g (Mercury- to Mars-size) planetary embryos in $\sim 10^5$ years (*6*); and (iii) giant impacts between embryos, resulting in full-size 10^{27} to 10^{28} g terrestrial planets in $\sim 10^8$ years (*7*). Farther out in the disk, the density of solids is enhanced with condensed ices and the embryos may be capable of reaching about 10 Earth masses (M_{\oplus}) in $\sim 10^6$ years. Upon reaching this mass, the bodies may begin accumulating $\sim 10^2 M_{\oplus}$ of disk gas to form giant planets like Jupiter and Saturn in $\sim 10^7$ years (*8*). This is the “core-accretion” mechanism of giant planet formation, referring to the growth of a solid core followed by accretion of gas.

The standard model was developed to help explain how planets could have formed around our isolated Sun. However, binary

stars are the most common outcome of the star formation process, and evidence exists for protoplanetary disks in young multiple-star systems (*9*). The end-state of planet formation in such systems has also been observed. Nearly 30% of the detected extrasolar planets exist in multiple-star systems (see Table 1).

The odd orbital characteristics of extrasolar giant planets are forcing considerable modifications to the standard model of planet formation. One suggestion is that giant planets like Jupiter may not form by core accretion but through a mechanism referred to as “disk instability” (*10*). Disk instability is a process involving gravitational collapse of Jupiter-mass clumps of gas and dust in a protoplanetary disk. Once an instability develops in the disk, formation of gravitationally bound giant gaseous protoplanets can occur on a time scale on the order of 100 years (*10*). This suggests that giant planets could have formed well before the runaway phase of growth of terrestrial planet embryos. The early evolution of planetesimals would then be dominated not by their own rather feeble mutual perturbations, but by much stronger perturbations from the massive planets.

As planetesimals orbit the central star, they are subject to gas drag from the protoplanetary disk. The gas in the disk is partially supported by its own pressure and orbits the star slightly slower than the Keplerian velocity. Planetesimals orbit with Keplerian velocity and, therefore, experience a head-wind drag force, the magnitude of which is inversely related to the

radius of the planetesimal (*11*). As the system evolves, secular perturbations from the massive companions act to increase planetesimal eccentricities (*e*) and inclinations (*I*) while the gas drag force dissipates orbital energy, damping *e* and *I* in a way that depends on planetesimal size (*12, 13*). Gas drag also removes angular momentum, causing planetesimal orbits to slowly decay toward the star. This size-dependent orbital decay slowly changes the relative orientation of planetesimal orbits as smaller bodies decay faster and overtake larger ones (*12*). A combination of secular perturbations and gas drag leads to a size-dependence in *e* and *I* (*12, 13*) as well as in the phasing of the orbital orientation angles [(*12*); see also fig. 9 in (*6*)]. The size-dependent phasing of orbital elements leads to low encounter velocities between similarly sized bodies and high encounter velocities between bodies of different size.

Full-scale simulations of planetesimal growth that include mutual perturbations, secular perturbations, and gas drag are beyond the reach of current techniques. Theoretically, one would need to include $\sim 10^{12}$ small ($\sim 10^{14}$ g) planetesimals to form a single 10^{26} g embryo. Direct *N*-body integrations of mutually perturbing planetesimals cannot even remotely approach this figure, treating only $\sim 10^4$ bodies over the time scale required. However, existing statistical simulations of planetary growth are not limited by the number of bodies. But these simulations assume that the orbits are completely randomized, so they cannot include the size-dependent orbital phasing. We have developed a hybrid approach that capitalizes on the strengths of each technique. We use *N*-body integration of nonperturbing planetesimals to map the size-dependent velocity distribution and statistical simulation to follow planetesimal growth. Mutual perturbations between planetesimals are not included.

For the *N*-body portion we used the Wisdom-Holman (*14*) symplectic integration technique as implemented by Levison and Duncan (*15*) and modified to include gas drag (*12, 16*). For the massive companions, we used Jupiter and Saturn with their present masses placed on orbits one astronomical unit (AU), the mean Earth-Sun distance, farther from the Sun than their current positions (i.e., Jupiter at 6.2 AU and Saturn at 10.5 AU). This was done to allow for later orbital mi-

¹Department of Astronomy, University of Maryland, 1204 CSS Building, Stadium Drive, College Park, MD 20742-2421, USA. ²Department of Terrestrial Magnetism, Carnegie Institution of Washington, 5241 Broad Branch Road, NW, Washington, DC 20015-1305, USA.

*To whom correspondence should be addressed. E-mail: kortenka@astro.umd.edu

REPORTS

gration of the planets by planetesimal scattering (17). All other initial orbital elements for the planets were equal to their present values, rendering this a fully three-dimensional simulation. Planetesimals were treated as massless test particles in the *N*-body routines but were assigned a mass for the gas drag effects. A total of 20,000 planetesimals were used, 500 for each 1/3 increment in log mass between 10^{13} and 10^{26} g. Initial orbits for the planetesimals were circular, coplanar (in the invariable plane of the two planets), and uniformly distributed between 0.5 and 4.0 AU. To maintain uniform coverage of this region, each time a planetesimal decayed inside 0.5 AU another was introduced at 4 AU. The nebular gas density at 1 AU was 1.18×10^{-9} g cm⁻³ (11) and followed a simple $1/r$ scaling of density with heliocentric distance *r*.

Encounter velocities were calculated for all intersecting orbits between 0.9 and 1.1 AU over the entire range of sizes. Figure 1 shows encounter velocities for 10^{25} g “target” bodies and equal or lesser size “projectile” bodies. Velocity distributions similar to that shown in Fig. 1 are established within a few thousand years for the smallest targets and within a few tens of thousands of years for the largest targets. Once established, these distributions persist for the duration of the simulations, some of which lasted $\sim 10^6$ years. The distribution of encounter velocities is a critical factor that determines how a population of planetesimals will accumulate into larger bodies. High encounter velocities can actually lead to erosion of the target rather than growth. On the other hand, low encounter velocities can gravitationally enhance the cross-sectional area of the target (18) and cause rapid growth.

To model planetesimal growth, we used a semi-automated least-squares technique to fit a smooth function to 640 different velocity dis-

tributions that are similar to the one shown in Fig. 1. These velocity distributions covered all target sizes from 10^{13} to 10^{26} g at 16 different time-steps chosen to follow the velocity evolution. This process was performed four times for regions centered on 1, 1.5, 2, and 2.3 AU. The resulting 2560 time- and size-dependent velocity functions were used to calculate encounter velocities between all colliding planetesimals. We then applied the statistical growth algorithm described by Inaba *et al.* (19). The initial surface density of solids was 10 g cm⁻² at 1 AU, scaling with $r^{-3/2}$. Nebular gas density was left identical to the *N*-body value. Solid planetesimals had a density of 3 g cm⁻³, and all planetesimals had the same initial mass of 10^{14} g (corresponding to a radius of about 200 meters). Cratering and fragmentation were included using the methods described by Wetherill and Stewart (20). Velocities for fragments smaller than 10^{13} g were extrapolated from the known distribution. Fragments below 10^7 g (≈ 1 meter) were immediately removed from the simulations because we presume they are lost rapidly by gas drag.

A separate growth simulation was performed in each region, and the width of each zone was 0.2 times the mean distance, or 0.2, 0.3, 0.4, and 0.46 AU, respectively. In all four regions, the growth is characterized as “orderly” [nonrunaway, see (1)] until the distribution reaches about the size of the largest asteroid, 1 Ceres ($\sim 10^{24}$ g) (Fig. 2). The distribution then becomes bimodal, transitioning to runaway growth (5) and producing Mercury- to Mars-size embryos. All planetesimals were assumed to be uniformly distributed across a region, and embryos separated by more than 10 mutual Hill radii were considered dynamically isolated (21) and were not allowed to collide. This resulted in multiple runaway embryos emerging in each region (Fig. 2).

Note that mutual perturbations between planetesimals are not included in these calculations. An alternative form of runaway

Table 1. Planets in multiple-star systems (28).

System name	No. of planets	No. of stars
HD13445 (Gliese 86)	1	2
HD19994 (94 Ceti)	1	2
HD27442 (ϵ Ret)	1	2
HD57819 (<i>v</i> And)	3	2
HD75732 (55 Canc)	2	2
HD80606	1	2
HD120136 (τ Boo)	1(2)	2
HD121504	1	2
HD143761 (ρ Cor Bor)	1	2
HD168443	1	2
HD178911	1	3
HD186427 (16 Cyg)	1	3
HD192263	1	2
HD195019	1	2
HD213240	1	2
HD217107	1(2)	2
PSR1257+12	3(4)	1
PSR1620-26	1	2

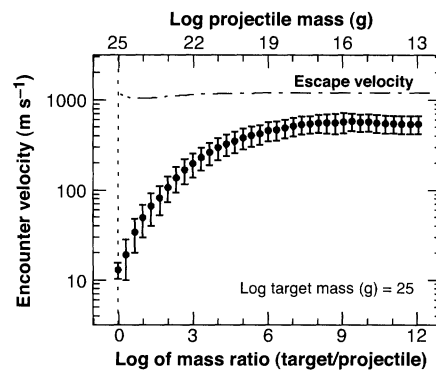


Fig. 1. Planetesimal encounter velocities near 1 AU with respect to 10^{25} g target bodies during the time interval from 150 to 175 thousand years (ky). The points are the mean velocity and error bars are ± 1 standard deviation. The combined surface escape velocity of the target and projectile is indicated by the horizontal dashed line.

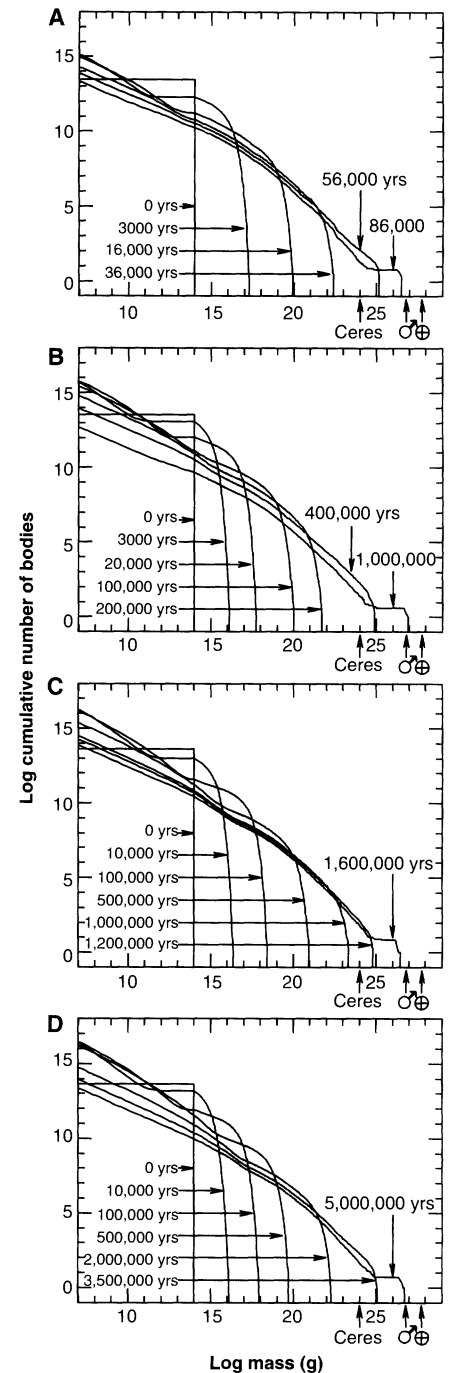


Fig. 2. Growth of planetesimals subject to nebular gas drag and secular perturbations from massive bodies. Initially all planetesimals have identical masses of 10^{14} grams. Growth is calculated in four different regions centered on 1, 1.5, 2, and 2.3 AU (A through D, respectively). Beyond 2.3 AU, growth is severely limited by the effects of strong resonances with the massive bodies. The masses of Earth (⊕), Mars (♂), and the largest asteroid (Ceres) are indicated for comparison. Note that these plots are on a log-log scale and that multiple embryos emerge in each region.

growth arises when secular perturbations and gas drag act together to establish size-dependent encounter velocities that remain low when colliding bodies are of similar size. Collisions between bodies of markedly different size are at high velocity and can lead to cratering and erosion, but our simulations show that growth overcomes erosion (Fig. 2). This general result should apply regardless of whether the perturbations are from Jupiter-like companions formed earlier by disk instability, stellar-mass objects in multiple-star systems, or short-lived instabilities that lead to asymmetries in the massive protoplanetary disk. We propose classifying this new form of runaway growth as "Type II."

Classical "Type I" runaway growth occurs in a self-gravitating population of planetesimals. Random orbital kinetic energy is exchanged during gravitational encounters between large and small bodies, and the population trends toward energy equipartition, a process dubbed "dynamical friction" (22). Dynamical friction lowers the encounter velocities of the larger bodies with respect to each other, enhancing their effective collision cross-sections and increasing the rate at which they accumulate each other. Under these conditions, nearly the entire growth period up to embryo size is in Type I runaway mode. In our simulations, which are not self-gravitating, the size-dependent phasing of orbital elements holds encounter velocities low between all similar-size bodies (typically 1 to 10 m s^{-1}) (Fig. 1). Initially, these encounter velocities exceed the planetesimal escape velocities so there is no enhancement of collision cross sections and growth is orderly. As larger and larger bodies grow, their escape velocities approach and then exceed the relatively low encounter velocities, causing the transition from orderly growth to Type II runaway growth. In this way, the effects of dynamical friction are mimicked by the size-dependent phasing of orbital elements.

Our attempts at including self-gravitating planetesimals (23) indicate that when the distribution reaches 10^{24} to 10^{25} g the mutual perturbations are beginning to become important, although they are still dominated by the size-dependent phasing of secular perturbations. This suggests that just as Type II runaway is getting under way, the population may begin a transition to Type I runaway or evolve by some combination of the two. A more rigorous treatment using hardware and software capable of efficiently handling a very large number of self-gravitating bodies (24, 25) could confirm this. The identification of Type II runaway growth suggests that planetary bodies can form in environments in which protoplanetary orbits may have higher eccentricities and inclinations than are usually considered. In addition to the Solar System model we provide here, other examples in-

clude young multiple-star systems and the post-supernova environment in binary-pulsar systems.

References and Notes

1. V. S. Safronov, *Evolution of the Protoplanetary Cloud and Formation of the Earth and Planets* (Nauka, Moscow, Russia, 1969) [translated for NASA and NSF by Israel Program for Scientific Translation, 1972; NASA TT F-677].
2. V. Mannings, A. P. Boss, S. S. Russell, Eds., *Protostars and Planets IV* (Univ. of Arizona, Tucson, AZ, 2000).
3. R. M. Canup, K. Righter, Eds., *Origin of the Earth and Moon* (Univ. of Arizona, Tucson, AZ, 2000).
4. S. J. Weidenschilling, J. N. Cuzzi, in *Protostars and Planets III*, E. H. Levy, J. I. Lunine, Eds. (Univ. of Arizona, Tucson, AZ, 1993), pp. 1031-1060.
5. Runaway growth, although it implies rapid growth, describes a process whereby a single dominant body grows more rapidly than the next largest bodies in the population. Typically, in a narrow accumulation zone, the final mass of the runaway embryo is two or three orders of magnitude larger than the next largest body, resulting in a bimodal mass distribution. The characteristics of runaway growth have been corroborated by several different methods; see the review by Kortenkamp *et al.* (6) and the recent contribution of Inaba *et al.* (19).
6. S. J. Kortenkamp, E. Kokubo, S. J. Weidenschilling, in (3), pp. 85-100.
7. R. M. Canup, C. B. Agnor, in (3), pp. 113-129.
8. G. Wuchterl, T. Guillot, J. J. Lissauer, in (2), pp. 1081-1109.
9. R. D. Mathieu, A. M. Ghez, E. L. N. Jensen, M. Simon, in (2), pp. 703-730.
10. A. P. Boss, *Astrophys. J. Lett.* **536**, 101 (2000).
11. I. Adachi, C. Hayashi, K. Nakazawa, *Prog. Theoret. Phys.* **56**, 1756 (1976).
12. S. J. Kortenkamp, G.W. Wetherill, *Icarus* **143**, 60 (2000).
13. F. Marzari, H. Scholl, *Astrophys. J.* **543**, 328 (2000).
14. J. Wisdom, M. Holman, *Astron. J.* **102**, 1528 (1991).
15. H. F. Levison, M. J. Duncan, *Icarus* **108**, 18 (1994).
16. R. Malhotra, *Celes. Mech. Dynamic. Astron.* **60**, 373 (1994).
17. R. Malhotra, *Nature* **365**, 819 (1993).
18. E. J. Öpik, *Proc. Irish Acad.* **54**, 165 (1951).

19. S. Inaba, H. Tanaka, K. Nakazawa, G. W. Wetherill, E. Kokubo, *Icarus* **148**, 235 (2001).
20. G. W. Wetherill, G. R. Stewart, *Icarus* **106**, 190 (1993).
21. J. E. Chambers, G. W. Wetherill, A. P. Boss, *Icarus* **119**, 261 (1996).
22. G. R. Stewart, W. M. Kaula, *Icarus* **44**, 154 (1980).
23. S. J. Kortenkamp, G. W. Wetherill, *Lunar Plan. Sci. Conf.* **31** (abstr. 1813) (2000).
24. E. Kokubo, S. Ida, *Icarus* **131**, 171 (1998).
25. D. C. Richardson, T. Quinn, J. Stadel, G. Lake, *Icarus* **143**, 45 (2000).
26. R. P. Butler *et al.*, *Astrophys. J.* **526**, 916 (1999).
27. M. C. Miller, D. P. Hamilton, *Astrophys. J.* **550**, 863 (2001).
28. Table 1 was compiled from J. Schneider's Extra-solar Planets Catalog (www.obspm.fr/encycl/catalog.html) by searching the SIMBAD database (<http://simbad.u-strasbg.fr/sim-fid.pl>) for the name of each star under "confirmed planets." Systems are listed in order of their Henry Draper (HD) catalog numbers with alternative names in parentheses. Some binary designations listed with SIMBAD have been questioned and may not be binaries, such as ν And (26). Also, some binaries are not obviously denoted in SIMBAD, such as 55 Cancri, but are described as binaries or multiples in the planet discovery papers cited in the Extra-solar Planets Catalog. One of the stars in HD168443 is a ≥ 17 Jupiter-mass "brown dwarf." Some binaries listed have very wide separations and may not have a direct influence on formation of terrestrial planets. Numbers in parentheses indicate that an additional planet is suspected in the system. The last two entries in the table are for the terrestrial-size pulsar planets. Millisecond pulsars are conventionally considered to have been spun-up by mass accretion from a stellar companion, which may or may not still reside in the system [although this theory has been recently questioned, see (27)]. The 18 systems in Table 1 include roughly 30% of the detected extrasolar planets orbiting in 60 different star systems as of 1 May 2001.
29. We are grateful to J. Chambers for the use of his *N*-body code, a recent version of which can be downloaded from <http://star.arm.ac.uk/~jec/>. We also thank A. Boss, D. Hamilton, and two anonymous reviewers for their helpful comments.

9 May 2001; accepted 10 July 2001

Molecular Evidence for the Early Colonization of Land by Fungi and Plants

Daniel S. Heckman,¹ David M. Geiser,² Brooke R. Eidell,¹ Rebecca L. Stauffer,¹ Natalie L. Kardos,¹ S. Blair Hedges^{1*}

The colonization of land by eukaryotes probably was facilitated by a partnership (symbiosis) between a photosynthesizing organism (phototroph) and a fungus. However, the time when colonization occurred remains speculative. The first fossil land plants and fungi appeared 480 to 460 million years ago (Ma), whereas molecular clock estimates suggest an earlier colonization of land, about 600 Ma. Our protein sequence analyses indicate that green algae and major lineages of fungi were present 1000 Ma and that land plants appeared by 700 Ma, possibly affecting Earth's atmosphere, climate, and evolution of animals in the Precambrian.

Plants, animals, and fungi are well adapted to life on land, but the first colonists faced a harsh physical environment (1, 2). The establishment of terrestrial eukaryotes may have been possible only through associations between a fungus and a phototroph (3, 4). The

most widespread of these symbioses today are lichens and arbuscular mycorrhizae. The former consist of cyanobacteria or green algae and ascomycotan (or more seldom, zygo- or basidiomycotan) fungi, and the latter join a plant with a glomalean fungus (4). It is un-